

## *Supplementary Material*

### **Photoluminescent sea urchin-shaped carbon nanobranched polymers as nanoprobe for selective and sensitive assay of hypochlorite**

Xin Zhang<sup>1,2</sup>, Jian Qu<sup>1,\*</sup>, and Shou-Nian Ding<sup>2,\*</sup>

*<sup>1</sup>School of Materials Science and Engineering, Yancheng Institute of Technology,  
Yancheng 224051, China*

*<sup>2</sup>School of Chemistry and Chemical Engineering, Southeast University, Nanjing  
211189, China.*

\*Corresponding authors: (J. Qu) iamqujian@ycit.edu.cn

(S.-N. Ding) snding@seu.edu.cn

## Contents

Chemicals and apparatus	S3
Figure S1. TEM of carbon-based nanomaterials from L-cysteine and uric acid	S5
Figure S2. XPS survey spectrum of SUCNPs	S5
Figure S3. Influences of pH and ionic strength on the FL	S6
Figure S4. Effect of pH on the analysis of $\text{ClO}^-$ using SUCNPs	S6
Figure S5. UV-vis spectra of SUCNPs solution with and without $\text{ClO}^-$ addition	S7
Figure S6. Influences of air exposure time (A), air exposure time (B), purging with $\text{O}_2$ (C) and daylight (D) on FL performance	S8
Figure S7. FL spectra of SUCNPs with the additions of different oxidants	S9
Calculation of detection limit	S11
Fig. S8 FL spectra of real samples with SUCNPs (20 $\mu\text{L}$ , 1.4 mg/mL) before and after addition of 30 nM $\text{ClO}^-$ .	S12

## Chemicals and apparatus

Uric acid ( $\geq 98\%$ ) was bought from Sigma-Aldrich. L-cysteine ( $\geq 98.5\%$ ) and sodium hypochlorite aqueous solution ( $\text{NaClO}$ , 8%) were offered by Sinopharm Chemical Reagent Co., Ltd. Phosphate buffer solution (50 mmol/L) was prepared with  $\text{Na}_2\text{HPO}_4$  and  $\text{NaH}_2\text{PO}_4$  just before measurement. Whatman chromatography paper #1 (Cat No. 3001-931, 58.0 cm x 68.0 cm) was obtained from GE Healthcare and cut into A4 size before use.

The UV-vis spectra were recorded by Shimadzu UV-2600 spectrophotometer (Japan). The FL spectra were collected by Fluoremax-4 spectrofluorometer (Horiba, USA). FL lifetime was tested with FluoroLog 3-TSCPC (Horiba Jobin Yvon Inc., Japan), and the decay curves were fitted with a biexponential function. The absolute photoluminescence quantum yield (PLQY) was directly measured and calculated using a quantum yield accessory (Horiba Jobin Yvon Inc.). The morphology of SUCNPs was taken with high resolution transmission electron microscopy (HRTEM, JEM-2100, JEOL, Japan). Fourier transform infrared (FR-IR) spectrum was recorded using a Nicolet 5700 IR spectrometer (Thermo Nicolet Corporation, USA) in the range of 400-4000  $\text{cm}^{-1}$ . The Raman spectrum was measured from Thermo Scientific DXRxi Raman spectrometer (USA) with excitation wavelength at 532 nm. Powder X-ray diffraction (XRD) data was collected using a Bruker D8 discover X-ray diffractometer (Bruker, Germany). X-ray photoelectron spectroscopy (XPS) analysis was carried out on a Thermo ESCALAB 250 X-ray photoelectron spectrometer (Thermo Scientific, USA). Dynamic light scattering (DLS) tests were executed at 25°C on Malvern Zetasizer

(Nano ZS). The microfluidic paper analytical devices ( $\mu$ PADs) were designed using Adobe Illustrator CS6 software, and the wax pattern was printed on the chromatography paper as hydrophobic boundaries using a Xerox wax printer (ColorQube 8580).

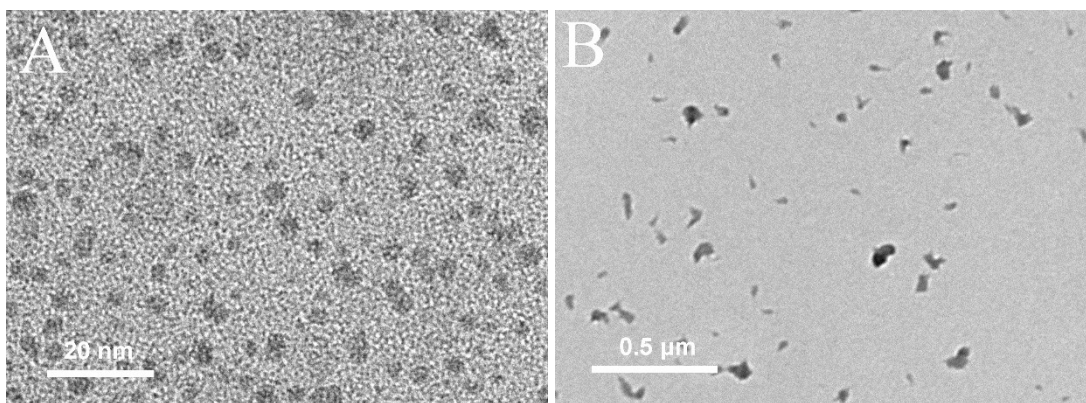


**Figure S1.** TEM images of N, S-doped carbon dots from cysteine (A) and carbon nanoribbons from uric acid (B).

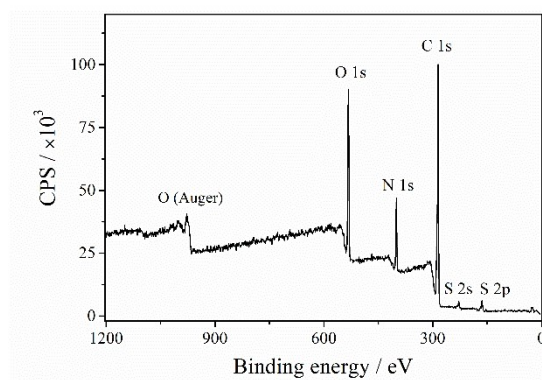


**Figure S2.** XPS survey spectrum of SUCNPs.

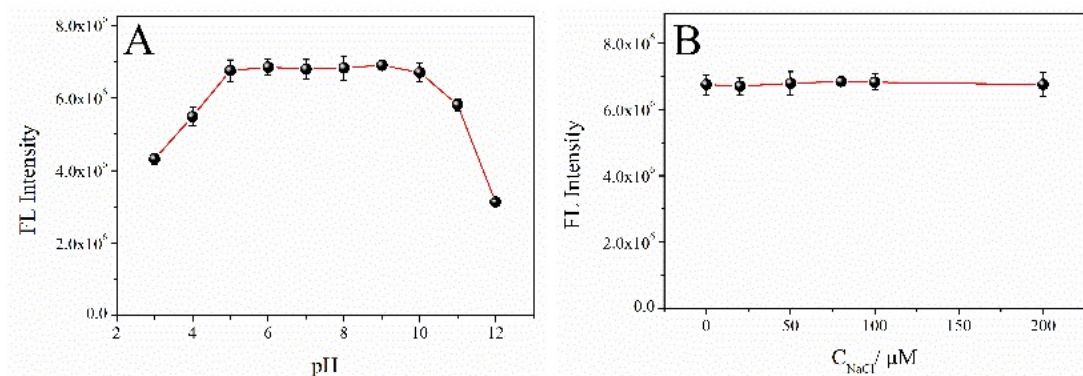


**Figure S3.** Influences of pH (A), ionic strength (B) on the FL intensity of the SUCNPs at 436 nm ( $\lambda_{ex}=350$  nm). Both the excitation and emission slit widths were 2 nm. Each RSD was lower than 5.33%.

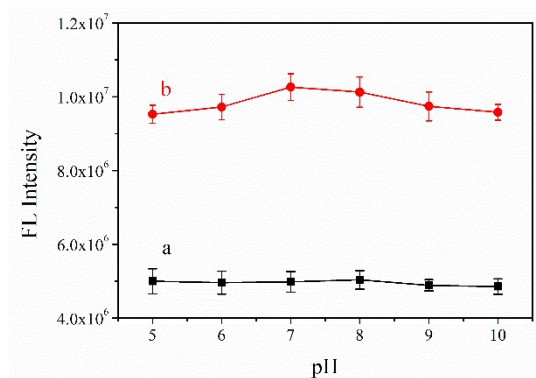


**Figure S4.** FL intensity of SUCNPs at the emission wavelength of 436 nm before (a) and after addition of  $500 \mu M ClO^-$  (b).  $\lambda_{ex}=350$  nm, both the excitation and emission slit widths were 2 nm. Each RSD was lower than 6.80%.

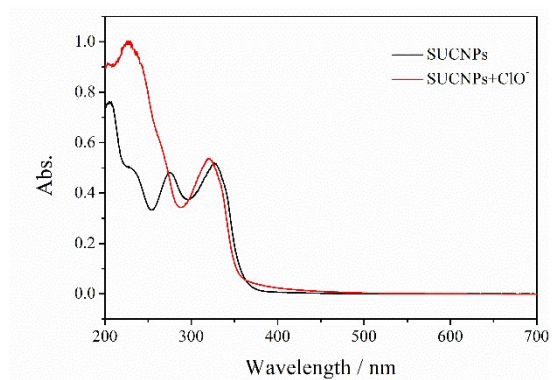


**Figure S5.** UV-vis spectra of the SUCNPs solution before and after addition of ClO<sup>-</sup> (the concentration of ClO<sup>-</sup> used is 200  $\mu$ M)

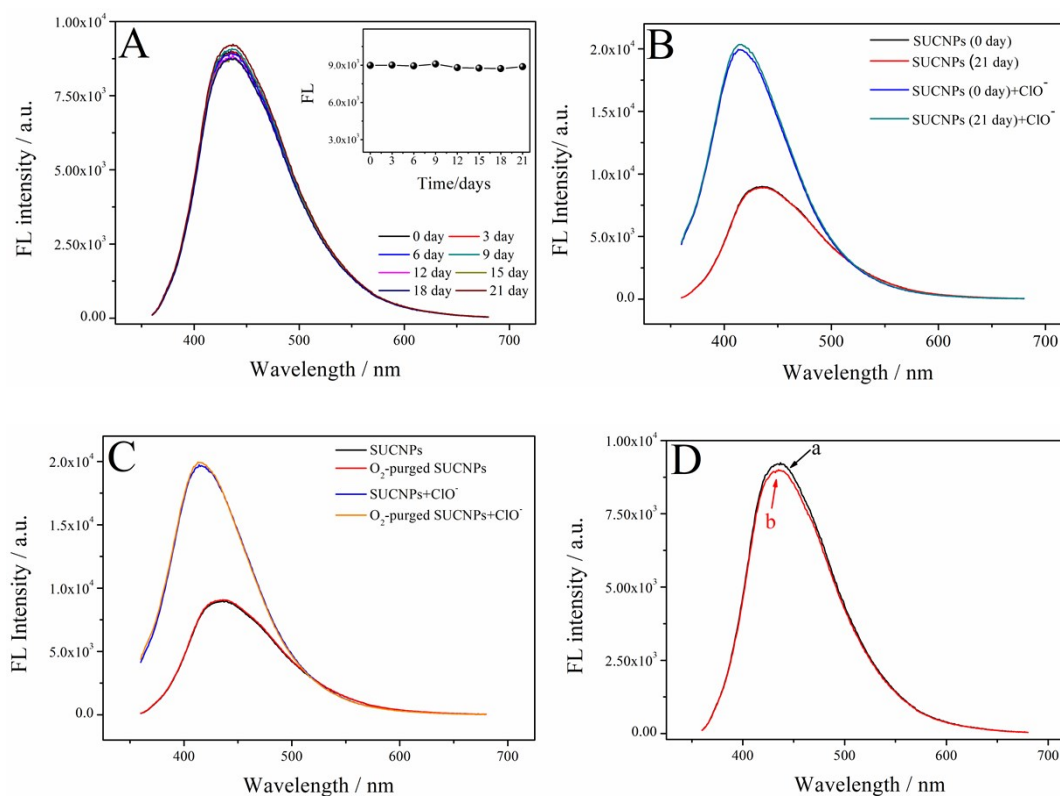


Fig. S6 FL spectra of SUCNPs solution exposed in the air for 21 days (A) and influence of air exposure time on the FL intensity of the SUCNPs at 436 nm ( $\lambda_{ex}=350$  nm, inset of A); FL spectra of SUCNPs solution (0 day) and the SUCNPs solution after 21-days air exposure with and without the treatment of 200  $\mu$ M  $\text{ClO}^-$  (B); FL spectra of SUCNPs solution and  $\text{O}_2$ -purged SUCNPs solution with and without the treatment of 200  $\mu$ M  $\text{ClO}^-$  (C); FL spectra of SUCNPs solution exposed under daylight before (a) and after (b) 2-months storage (D).



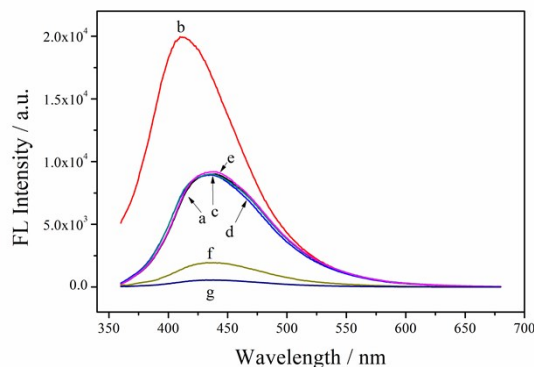


Fig. S7 FL spectra of SUCNPs solution (a) with the additions of  $\text{ClO}^-$  (b),  $\text{ClO}_2^-$  (c),  $\text{ClO}_4^-$  (d), NO (e),  $\text{H}_2\text{O}_2$  (f) and  $\cdot\text{OH}$  (g). The corresponding test conditions were similar to above measurements.

According to the CRC Handbook of Chemistry and Physics (90 th edition, edited by D. R. Lide et al.),<sup>1</sup> in an acidic environment:  $E^\ominus(\text{ClO}^-, \text{H}^+ | \text{Cl}_2) = 1.611 \text{ V} > E^\ominus(\text{ClO}_2^-, \text{H}^+ | \text{Cl}_2) = 1.57 \text{ V} > E^\ominus(\text{ClO}_3^-, \text{H}^+ | \text{Cl}_2) = 1.47 \text{ V} > E^\ominus(\text{ClO}_4^-, \text{H}^+ | \text{Cl}_2) = 1.39 \text{ V}$ ; in a basic environment:  $E^\ominus(\text{ClO}^- | \text{Cl}^-, \text{OH}^-) = 0.81 \text{ V} > E^\ominus(\text{ClO}_2^- | \text{Cl}^-, \text{OH}^-) = 0.76 \text{ V} > E^\ominus(\text{ClO}_3^- | \text{Cl}^-, \text{OH}^-) = 0.62 \text{ V} > E^\ominus(\text{ClO}_4^- | \text{Cl}^-, \text{OH}^-) = 0.36 \text{ V}$ . It is well-acknowledged that under the standard state, the higher standard electrode potential value is, the stronger the oxidizability of the oxide is. Thus, it could be inferred that the oxidizability sequence is  $\text{ClO}^- > \text{ClO}_2^- > \text{ClO}_3^- > \text{ClO}_4^-$ , whether in acidic or basic environment. Thus, the presences of  $\text{ClO}_2^-$  and  $\text{ClO}_4^-$  would not trigger the FL change as the  $\text{ClO}^-$  does. Similar phenomenon could be found in the previous report, in which  $\text{ClO}^-$  oxidized the reductive groups on the CDs, but  $\text{ClO}_2^-$  and  $\text{ClO}_3^-$  did not influence the FL of CDs.<sup>2</sup>

In contrast,  $\text{H}_2\text{O}_2$  and  $\cdot\text{OH}$  possess stronger oxidizability than  $\text{ClO}^-$  according to their higher standard electrode potentials ( $E^\ominus(\cdot\text{OH}, \text{H}^+ | \text{H}_2\text{O}) = 2.80 \text{ V} > E^\ominus(\text{H}_2\text{O}_2, \text{H}^+ | \text{H}_2\text{O}) = 1.776 \text{ V} > E^\ominus(\text{ClO}^-, \text{H}^+ | \text{Cl}_2) = 1.611 \text{ V}$ ). The presences of  $\cdot\text{OH}$  and  $\text{H}_2\text{O}_2$  caused FL quenching towards SUCNPs. It is assumed that a non-fluorescent complex or nanostructure might be formed under the stronger oxidation, rather than single oxidation of thioether by  $\text{ClO}^-$ . But this response would not influence the selectivity of

SUCNPs towards  $\text{ClO}^-$ . For one thing, the quantitation relationship is constructed based on the fluorescence ratio value of  $I_{401\text{nm}}/I_{436\text{nm}}$ . FL quenching would not affect this value. For another thing,  $\text{H}_2\text{O}_2$  cannot coexist with  $\text{NaClO}$  in a genuine sample because oxidation-reduction reaction would occur when they meet:  $\text{NaClO} + \text{H}_2\text{O}_2 \rightarrow \text{NaCl} + \text{O}_2\uparrow + \text{H}_2\text{O}$ .

### Calculation of detection limit

The detection limit was calculated based  $3\sigma/k$  according to previous literatures.<sup>3,4</sup> FL measurements for blank samples with five parallel tests first, which displayed average  $I_{401\text{nm}}/I_{436\text{nm}}$  value of 0.49257 with standard deviations ( $\sigma$ ) of  $2.3 \times 10^{-4}$ .

Blank samples	1	2	3	4	5
$I_{401\text{nm}}$	2545040	2457630	2444800	2473620	2468910
$I_{436\text{nm}}$	5170220	4990820	4961040	5021150	5010470
$I_{401\text{nm}}/I_{436\text{nm}}$	0.49225	0.49243	0.49280	0.49264	0.49275

Linear regression equation was fitted as  $I_{401\text{nm}}/I_{436\text{nm}} = 0.0226C(\text{ClO}^-, \mu\text{M}) + 0.5618$ ,  $k$  represents the slope of linear regression equation, equaling to 0.0226.

$$\text{Detection Limit (DL)} = \frac{3\sigma}{k} = \frac{3 \times 2.3 \times 10^{-4}}{0.0226} = 30.5 \text{ nM} \approx 30 \text{ nM}$$

### References

- [1] D. R. Lide. CRC Handbook of Chemistry and Physics, 90 th Edition, 2010.
- [2] L.-S. Li, X.-Y. Jiao, Y. Zhang, C. Cheng, K. Huang and L. Xu, *Sens. Actuators B.*, 2018, **263**, 426-435.
- [3] J. Qu, X. Zhang, Y. Liu, Y. Xie, J. Cai, G. Zha, S. Jing, *Microchim. Acta*, 2020, **187**, 355.
- [4] P. Chen, Z. Zheng, Y. Zhu, Y. Dong, F. Wang and G. Liang, *Anal. Chem.*, 2017, **89**, 5693-5696.

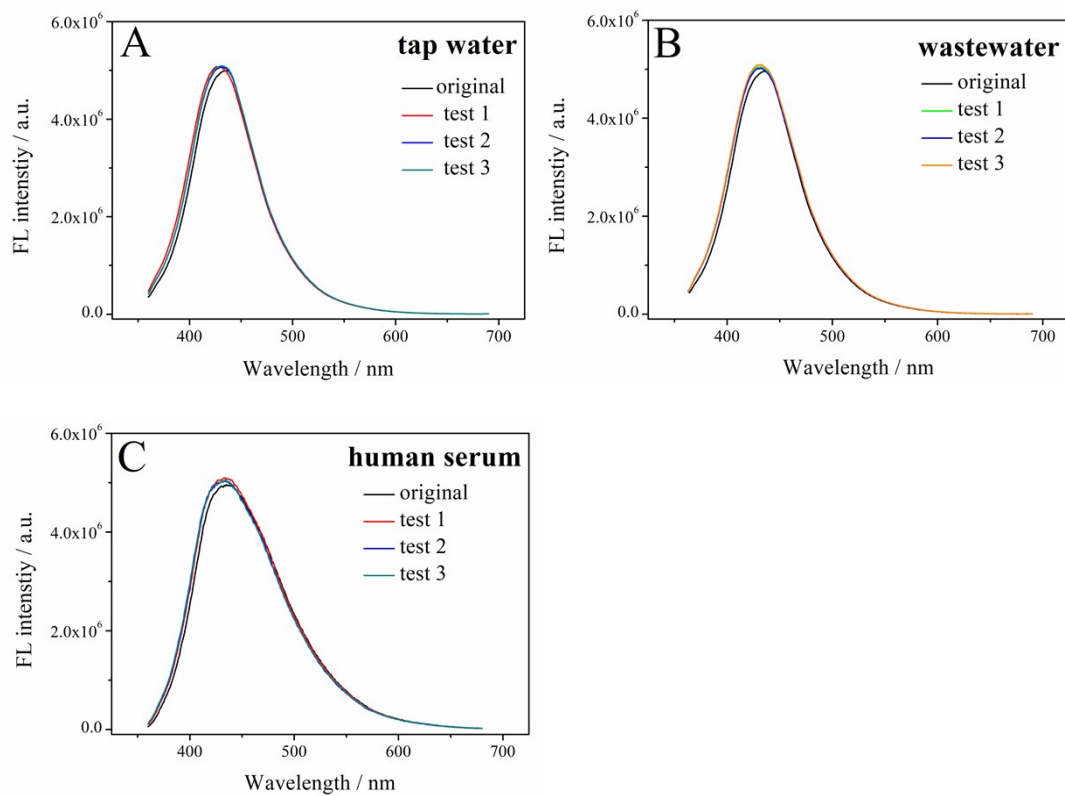


Fig. S8 FL spectra of real samples with SUCNPs (20  $\mu$ L, 1.4 mg/mL) before and after addition of 30 nM  $\text{ClO}^-$ . A: tap water, B: wastewater, C: human serum.